3D Volume Extraction of Densely Packed Cells in EM Data Stack by Forward and Backward Graph Cuts

Huei-Fang Yang and Yoonsuck Choe

***Abstract*— 3D reconstruction on dense nanoscale medical images is a very challenging research topic. The challenge comes from the fact that boundaries of objects on such images are not always very clear due to imperfect staining. This makes the segmentation of dense nanoscale medical images very difficult and thus increases the difficulty in 3D reconstruction. In this paper, we proposed a method based on watershed and an interactive segmentation technique, graph cuts, to extract 3D volumes from dense nanoscale medical images. In our method, images are first segmented by a marker-controlled watershed algorithm. Markers for watershed segmentation algorithm are seed points generated by using distance transform, followed by a new grouping method that clusters seed points that are too close. Regions obtained by watershed transform segmentation algorithms are considered as nodes in a graph. Edges are to connect between the nodes in adjacent image slices. The weight on each edge is defined based on the overlapped area between nodes. User-selected nodes (regions) in an initial image slice serve as hard constraints in the minimization process. A globally optimal 3D volume is obtained by minimizing MAP-MRF energy function via graph cuts. In our application, in order to obtain a complete 3D volume structures including branching, the final 3D volume is the union of two 3D volumes obtained by performing the minimization of MAP-MRF energy function using graph cuts forwards and backwards through the image stack. Experiments are conducted both on synthetic data and on nanoscale image sequences from the Serial Block Face Scanning Electron Microscope (SBF-SEM). The results show that our method can successfully extract 3D volumes.**

I. Introduction

Segmentation of medical images has drawn particular attention recently. One main reason is that huge amounts of medical images have been generated but it is very time-consuming for humans to delineate the boundaries manually, so reliable and fast segmentation algorithms are required to accomplish segmentation task as well as the subsequent 3D reconstruction work.

Segmentation of nanoscale images is a challenging task, especially nanoscale images generated by Serial Block Face Scanning Electron Microscopy (SBF-SEM) recently developed by Denk and Horstmann [7]. SBF-SEM data are a stack of 2D nanoscale medical images with a resolution on the order of ten nanometers. Denk and Horstmann developed SBF-SEM to enable high image resolution to make the identification of small organelles possible. Interstitial staining for SBF-SEM images highlight cell boundaries so that cells (foreground) are in brighter gray-scale intensity and non-cells (background) are in darker gray-scale intensity. Fig. 1 shows successive 2D images of the optic tectum of larval zebrafish. Segmentation of SBF-SEM images amounts to delineating cell boundaries. The challenges of identifying cell boundaries come from inevitable staining noise and weak or missing boundaries between cells that are located very close.

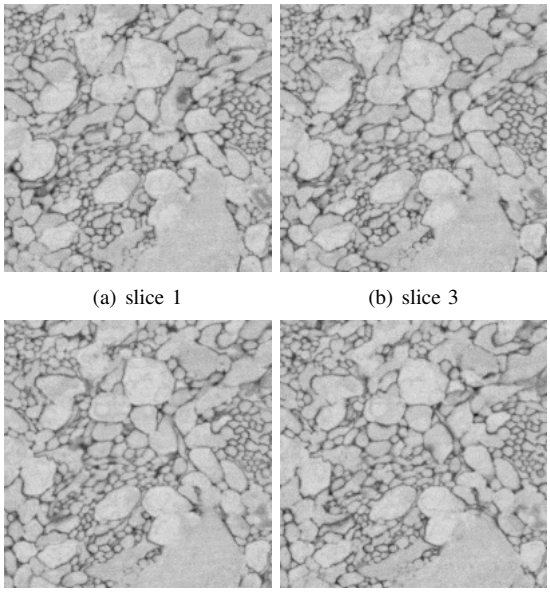

(a) slice 1 (b) slice 3

(c) slice 5 (d) slice 7

Fig. 1. Part of an SBF-SEM image stack.

Popular segmentation algorithms for medical images include thresholding [13], watershed [15], and active contours [5] [6] [16] [1]. Unfortunately, thresholding on SBF-SEM images cannot give satisfying segmentation results due to the incomplete boundaries and inhomogeneous staining intensities. Watershed segmentation algorithms partition an image into small regions with homogeneous intensities; however they suffer from the over-segmentation problem. Edge-based [5] [9] and region-based [6] active contour methods encounter the same problem as thresholding, i.e., being unable to correctly segment objects with missing boundaries. Weak or missing object boundaries in SBF-SEM images increase the difficulty of determining the correct boundaries. To untangle the problem with blurred boundaries between objects that are too close, one possible solution is user intervention. Interactive segmentation is becoming more popular since a perfect segmentation seems not possible by fully automated segmentation algorithms. One of the successful interactive segmentation methods is graph cuts [3] [2], which also have

Huei-Fang Yang and Yoonsuck Choe are with the Department of Computer Science and Engineering, Texas A&M University, College Station, TX, USA (email: hfyang@cs.tamu.edu, choe@tamu.edu).

been applied on 3D CT images to separate bones [10] and to segment liver tumors [12]. In graph cuts, users can roughly impose hard constraints. A globally optimal segmentation is obtained by the minimization of an energy function and satisfying user specified hard constraints at the same time. The merit of graph cuts is that user-specified hard constraints provide segmentation clues to the segmentation algorithms in order to achieve a more accurate segmentation result.

In this paper, we propose a segmentation method based on watershed and graph cuts to extract 3D volumes from SBF-SEM images. Our method takes advantage of watershed algorithms to produce over-segmented regions to overcome the weak or missing object boundaries problem. Also, instead of doing graph cuts on individual pixels, we do it on the watershed regions, thus decreasing computational complexity. We first generate seed points by using distance transform. Then, we introduce a new method to group the seed points. The idea of grouping seed points that are two close is based on expanded circles centered at seed points. Regions obtained by a marker-controlled watershed transform segmentation algorithm (using grouped seed points as markers) are considered as nodes in a graph. Edges are to connect between the nodes in adjacent image slices in the image stack. User-selected regions are set as hard constraints in the minimization process. A globally optimal segmentation of 3D volumes is then produced by graph cuts. In traditional graph cuts on foreground/background segmentation, intensities change between foreground objects and background. However, in our case, intensities between foreground and background are sometimes very similar due to missing object boundaries and watershed over-segmented regions have very similar intensities also. Therefore, the novelty of our method is that the weighting function we defined does not rely on intensity information but depends on the overlapped area between nodes. We will elaborate this point in Section III.

The remainder of this paper is organized as follows. In section II, the method for preprocessing, including seed point generation, seed point grouping and marker-controller watershed algorithm, is introduced. In section III, method on 3D volume extraction from SBF-SEM images by graph cuts is presented. Section IV shows the experimental results on synthetic data and SBF-SEM data. Then section V provides the discussion of our work, followed by a conclusion and future work in section VI.

II. Preprocessing

A. Noise Removal

Gray-scale SBF-SEM images are first converted to binary images by Otsu's thresholding method [11], which are then used to compute distance transform images for seed point generation in the next step. The intensity values of objects on SBF-SEM images are inhomogeneous, and as a result small unnecessary objects can be generated after thresholding. To get rid of such unnecessary objects, we simply filtered out the objects by their size (area). Assume that S_f denotes the size of a foreground object, and if

$$S_f > T_f, \tag{1}$$

where T_f is a user-defined threshold value, we keep the object; otherwise, the object is considered as background. Similarly, for a non-object region, if its size S_b is greater than a threshold T_b, we keep it; otherwise, it is considered as foreground. Threshold values of T_f and T_b are determined empirically. Fig. 2(b) shows the noise removed binary image of fig. 2(a).

B. Seed Point Generation

The idea of generating seed points is to utilize distance transform on binary images. Seed points generated in this step are marker candidates needed for the marker-controlled watershed algorithm. The method to generate seed points is to apply distance transform on binary images followed by morphological reconstruction by geodesic dilation [14]. Assume that D is the distance transform image of the original image I, as shown in fig. 2(c). The marker image is $M = D - h$, where h is a pre-defined value. In our experiments, h was set to 10. The geodesic dilation of size 1 of the marker image M with respect to mask image D with structuring element B is defined as:

$$\delta^{(1)}(M) = (M \oplus B) \cap D, \tag{2}$$

where $\oplus$ denotes the dilation of M with structuring element B and $\cap$ is the point-wise minimum operation. The morphological reconstruction by geodesic dilation with size n is to perform the morphological reconstruction by geodesic dilation n times and is defined as:

$$\delta^{(n)}(M) = \underbrace{\delta^{(1)}(M) \circ \delta^{(1)}(M) \circ \cdots \circ \delta^{(1)}(M)}_{n \text{ times}}. \tag{3}$$

Finally, the seed points S of the original image I are obtained by computing regional maxima of $D - \delta^{(n)}(M)$:

$$S = \text{regionalmax}\left(D - \delta^{(n)}(M)\right). \tag{4}$$

Note that [14] proposed a sequential reconstruction algorithm to obtain $\delta^{(n)}(M)$. In that algorithm, instead of specifying the structuring element B explicitly, a neighborhood system should be determined. In our case, an 8-connected neighborhood system is used. The sequential reconstruction algorithm repeatedly scans an image in raster order and anti-raster order until stability so the value of n does not needed to be determined. Fig. 2(d) shows the generated seed points.

C. Seed Point Grouping

The objective of seed point grouping is to cluster very close seed points generated from the method above. We expand the generated seed points into circles first and if an overlapped area exists between the expanded circles, the seed points of those expanded circles are considered to belong in the same cluster. Let S_m and S_n be two seed points, and let r_m and r_n represent the distance from S_m and S_n to their boundaries, respectively. Now assume that C_m and C_n are

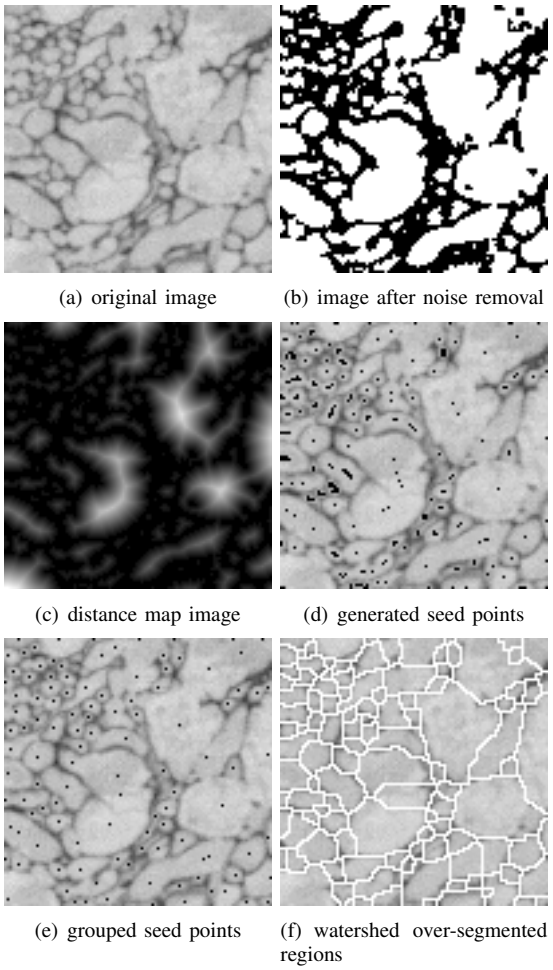

(a) original image (b) image after noise removal

(c) distance map image (d) generated seed points

(e) grouped seed points (f) watershed over-segmented regions

Fig. 2. Intermediate results of pre-processing process applied on an image.

two circles drawn from seed points S_m and S_n with radii r_m/a and r_n/a, where a is a positive constant. We say seed points S_m and S_n are in the same cluster, if

$$C_m \cap C_n \neq 0. \tag{5}$$

In our experiments, the value of a was set to 4. Fig. 2(e) shows the grouped seed points. The grouped seed points serve as makers for the subsequent watershed transform segmentation.

D. Marker-Controlled Watershed Transform Segmentation

The watershed transform algorithm [15] usually produces small regions with similar properties, such as similar intensities or textures of an image. In our method, instead of applying an unsupervised watershed transform algorithm of morphological gradient on SBF-SEM images, we used the grouped seed points introduced above as markers in the watershed transform segmentation of distance transform to obtain small regions. The small regions generated in this way retain the contour information as that in the original image. The result of marker-controlled watershed transform using grouped seed points as markers is shown in fig. 2(f).

III. 3D Volume Extraction

A. Graph Cuts

3D volume extraction, similar to foreground/background segmentation in 2D images, can be considered as a binary labeling problem. Assume that an image is represented as a graph $G =< V, E, W >$ with a set of nodes V representing pixels or image regions, a set of edges E connecting nodes and W are the weights assigned to edges. The binary labeling problem is to assign each node i with a unique label x_i, that is, $x_i \in \{0\,(\text{background}), 1\,(\text{foreground})\}$ such that $X = \{x_i\}$ minimizes the following energy function [8]:

$$E(X) = \lambda \cdot E_1(X) + E_2(X) \tag{6}$$

where

$$E_1(X) = \sum_{i \in V} E_i(x_i) \ \text{(regional term)} \tag{7}$$

$$E_2(X) = \sum_{\{i,j\} \in N_i} w_{i,j} \cdot \delta(x_i, x_j) \ \text{(boundary term)} \tag{8}$$

where N_i is the neighbors of node i, and the indicator function $\delta(x_i, x_j)$ is defined as:

$$\delta(x_i, x_j) = \begin{cases} 1 & \text{if } x_i \neq x_j \\ 0 & \text{if } x_i = x_j \end{cases}$$

The regional term, $E_i(x_i)$, indicates the cost when a label x_i is assigned to a node i. The boundary term, $E_2(X)$ captures the cost when nodes i and j are assigned different labels, i.e., there is a discontinuity between nodes i and j. The binary labeling problem described above is posed as a Maximum A Posteriori estimation of a Markov Random Field (MAP-MRF). [3] [2] proposed a combinatorial optimization framework based on s/t graph cuts to solve the minimization problem in equation (6) for foreground/background segmentation. S and T are two additional nodes denoting a foreground terminal (a source S) and a background terminal (a sink T), respectively. For more information as to how to formulate the minimization problem and to solve it, please refer to [3] [2] [4]. Here, we concentrate on how to define the E_1 and E_2 terms based on our application.

1) Data Term: In most cases, $E_i(x_i)$ defines the cost of node i belonging to the foreground or the background according to the intensity similarity. However, in our case, the obtained regions have very similar gray-scale intensities and so it is hard to define the cost according to the regional gray-scale intensities. As a result, instead of defining $E_i(x_i)$ based on regional gray-scale intensities, $E_i(x_i)$ therefore is defined based on which regions users would like to get the 3D volume from. In other words, users indicate a set of nodes (regions) i from the first image slice for 3D volume extraction. Those user-selected nodes are considered as foreground (F) and the costs of the selected nodes when they are assigned to foreground label are set to ∞. On the other hand, the rest of the regions in the first image slice are all considered as background (B) and the costs of these

nodes when they are assigned to background label are ∞. The definition of $E_i(x_i)$ is:

$$\begin{cases} E_i(x_i=1)=\infty & E_i(x_i=0)=0 & \forall i \in F \\ E_i(x_i=1)=0 & E_i(x_i=0)=\infty & \forall i \in B \\ E_i(x_i=1)=0 & E_i(x_i=0)=0 & \forall i \in U \end{cases} \quad (9)$$

where U indicates the other nodes not in the first image slice.

2) Boundary Term: Although our nodes are regions obtained from the watershed transform segmentation, a region adjacency graph between regions within 2D image slices is not used when constructing the graph. In our application, edges connect between nodes i and j if and only if an overlapped area exists between node i and node j, and nodes i and j are in adjacent images t and $t+1$, respectively. That is, edges only connect nodes between image slices, not nodes within the same image slice. Two over-segmented images are shown in fig. 3(a) and fig. 3(b) for image slices t and $t+1$, respectively. Fig. 3(c) shows the constructed graph for a set of specific regions in fig. 3(a) and fig. 3(b). Different from other methods defining edge weights based on gray-scale intensities to indicate boundary discontinuities, we define the weight of an edge $w_{i,j}$ between two nodes, i and j, according to the size of the overlapped area between them. The cost $w_{i,j}$ is defined as:

$$w_{i,j} = \exp\left(-\frac{(1-O_{i,j})^2}{2\sigma^2}\right) \quad (10)$$

where $O_{i,j}$ denotes the area overlap ratio of two nodes, i and j, i.e., let A_i and A_j represents the area of nodes i and j, respectively, and $A_{i,j}$ indicate the overlapped area between nodes i and j. $O_{i,j}$ is defined as:

$$O_{i,j} = \min\left(A_{i,j}/A_i, A_{i,j}/A_j\right), \quad (11)$$

The above equation penalizes a lot for edges with larger overlapped area between nodes while it penalizes less for those with smaller overlapped area between nodes. Also note that in our method, edges between nodes i and j are undirected, that is, $w_{i,j}$ equals to $w_{j,i}$.

B. Forward and Backward 3D Volume Extraction by Graph Cuts

Branching of cells is a common property in SBF-SEM images. The proposed method to extract 3D volumes should be able to handle cell branching. As mentioned above, the foreground nodes are those chosen by a user from the first image slice and others in the first images are set as background. Because of these settings, our method can handle regions that branch out (cell branching out), but cannot handle the case where multiple regions are merged together. To overcome this problem, a two-pass graph cuts on the minimization of an energy function are applied. After minimizing equation (6) by graph cuts in the forward direction, a backward direction of the minimization of equation (6) is also performed. The setting of nodes to either foreground or background in the backward graph cuts is similar to that of the forward graph cuts except that foreground nodes are now those regions in the last image slice obtained by forward graph cuts, and background nodes are those not extracted by the forward graph cuts. After the two-pass forward and background graph cuts are performed, two 3D volumes are obtained. The final 3D volume is the union of these two 3D volumes.

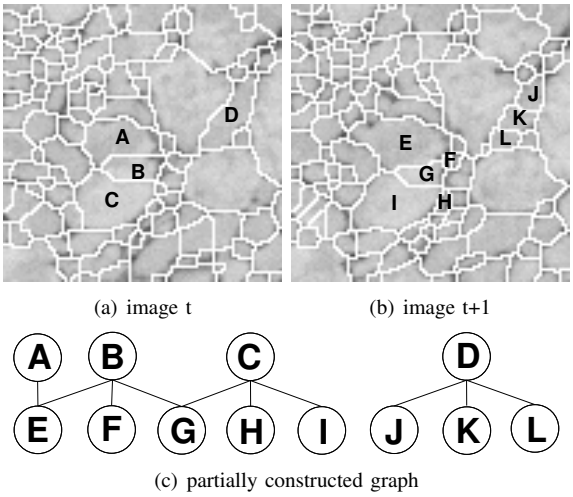

(a) image t (b) image t+1

(c) partially constructed graph

Fig. 3. Graph construction between two adjacent image slices. Letters in fig. 3(a) and fig. 3(b) denote over-segmented watershed regions. Two regions in adjacent images are connected if an overlapped area exists between them. For example, regions A and E have an overlapped area, a connection is built between them in the graph.

IV. Experimental Results

To show the ability of our method to extract 3D volumes from image stacks, we conducted experiments both on synthetic data and on SBF-SEM images.

A. Synthetic Data

The objective of experiments on synthetic data is to show the ability to extract 3D volumes, especially those with branches, so we generated a set of 2D image slices to simulate a particular 3D volume structure.

For cell branching, $100 \times 100 \times 100$ synthetic image slices are generated. Fig. 4 demonstrates the shape of the cell's structure at some image slices where a cell branches. The corresponding 3D volume structure obtained by our method is shown in fig. 5(a). Fig. 5(b) shows a more complicated 3D volume structure constructed from a stack of $300 \times 300 \times 100$ synthetic image slices where two branches are merged together and another branch emerge from the top of the sphere. The 3D volume extraction result shown in fig. 5(b) is the union of two 3D volumes obtained by the minimization of equation (6) by graph cuts, forward and backward.

B. SBF-SEM Images

SBF-SEM images are first pre-processed by the method mentioned in section II to obtain over-segmented watershed regions. A graph is constructed, considering those regions as nodes, and connected with edges between nodes in adjacent image slices. While constructing the graph, the weight of each edge is determined according to equation (10). In our

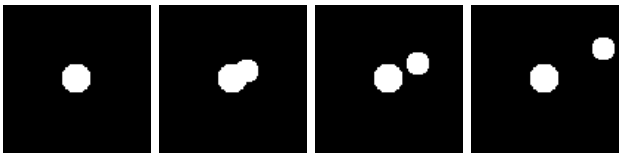

(a) slice 1 (b) slice 70 (c) slice 80 (d) slice 100

Fig. 4. 2D image slices of a branching cell.

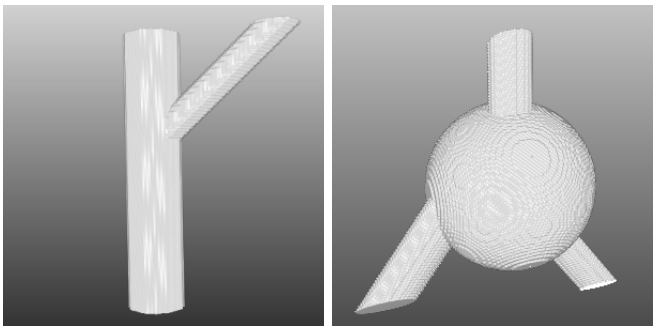

(a) (b)

Fig. 5. Extracted 3D volumes of synthetic data. (a) 3D reconstruction on a stack of $100 \times 100 \times 100$ images. (b) A more complicated 3D structure reconstructed from a stack of $300 \times 300 \times 300$ images.

experiments, the value of σ in equation (10) was set to 0.2. Users select nodes (regions) for 3D reconstruction and the costs of $E_i(x_i)$ are set based on equation (9). 3D volumes are then extracted based on the minimization of equation (6) according to user selected nodes (regions). Fig. 6 shows the extracted 3D volumes from SBF-SEM image slices. Fig. 6(c) demonstrates a case where a cell is branching. Fig. 6(e) shows the case where two cells are merged together. Fig. 6(a) and fig. 6(b) show the small bulb structures. As for fig. 6(d), it shows a larger extracted 3D volume structure.

V. Discussion

The main contribution of this paper is in its extension and integration of existing segmentation approaches for use in 3D reconstruction. We proposed novel methods for (1) seed point grouping for marker-based watershed, which provides different grouping range for each seed point rather than a single fixed grouping range for all the seed points (2) use of watershed regions instead of pixels, as nodes in graph cuts, which results in computational efficiency (3) graph construction by connecting between the nodes across images, not within images, and automatic determination of weight based on region overlap.

Our method takes user-selected nodes as hard constraints in the minimization process. In most cases, users only need to select the nodes from the first image slice and the rest of the 3D volumes are extracted. However, for some thin and elongated structures, more constraints are required. Another limitation is that in our current method, only a single 3D volume is extracted in a minimization process. To obtain multiple 3D volumes, users have to indicate nodes separately and run the two-pass graph cuts.

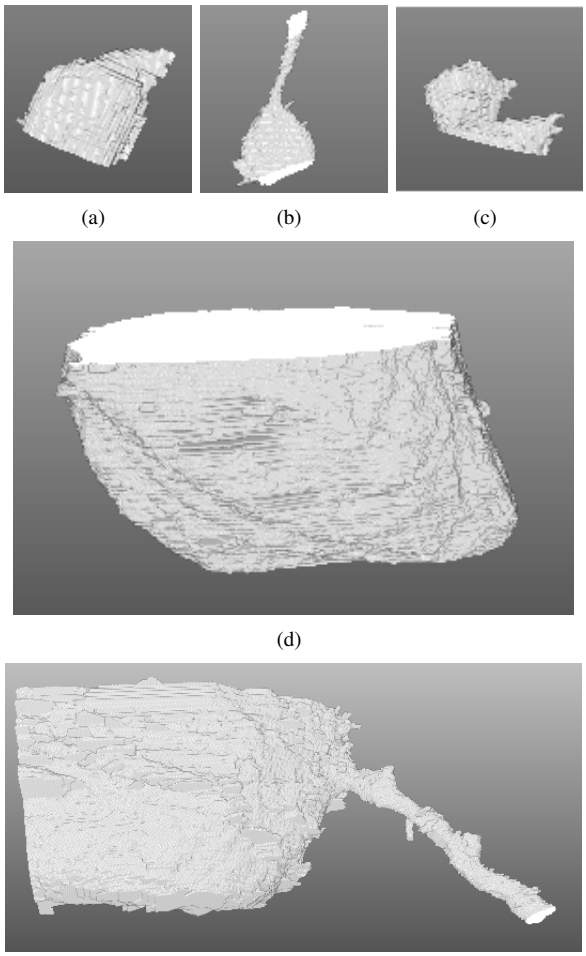

(a) (b) (c)

(d)

(e)

Fig. 6. Extracted 3D volumes from SBF-SEM data. (a) and (b) shows the small bulb structures. (c) demonstrates a case where a cell is branching. (d) shows a larger extracted 3D volume structure. (e) shows the case where two cells are merged together.

VI. Conclusion and Future Work

In this paper, we presented a segmentation method based on watershed and graph cuts to extract 3D volumes from SBF-SEM images. The use of watershed generated over-segmented regions as nodes in a graph instead of voxels not only speeds up the computation of MAP-MRF energy function, but also helps solve the missing or blurred boundary problem occurring in SBF-SEM images when the cross section regions are too close. We define the weights on edges between nodes based on the overlapped area information and perform two-pass (forward and backward) minimization using graph cuts to obtain the 3D volume structures according to the initial user input. Our method was tested on synthetic data and SBF-SEM images, and the results are very promising. Currently, our method extracts a single 3D volume structure for each minimization process. If the user wants to extract multiple 3D volume structures, our method needs to be initialized and performs the minimization process executed repeatedly. Future work will focus on extending

the current work to extract multiple 3D volume structures simultaneously.

REFERENCES

[1] P. S. Umesh Adiga. Segmentation of volumetric tissue images using constrained active contour models. *Computer Methods and Programs in Biomedicine*, 71(2):91–104, 2003.

[2] Yuri Boykov and Gareth Funka-Lea. Graph cuts and efficient n-d image segmentation. *International Journal of Computer Vision*, 70(2):109–131, 2006.

[3] Yuri Boykov and Marie-Pierre Jolly. Interactive graph cuts for optimal boundary and region segmentation of objects in N-D images. In *ICCV*, pages 105–112, 2001.

[4] Yuri Boykov and Vladimir Kolmogorov. An experimental comparison of min-cut/max-flow algorithms for energy minimization in vision. *IEEE Trans. Pattern Anal. Mach. Intell.*, 26(9):1124–1137, 2004.

[5] Vicent Caselles, Ron Kimmel, and Guillermo Sapiro. Geodesic active contours. *Int. J. Comput. Vision*, 22(1):61–79, 1997.

[6] Tony F. Chan and Luminita A. Vese. Active contours without edges. *IEEE Transactions on Image Processing*, 10(2):266–277, 2001.

[7] Winfried Denk and Heinz Horstmann. Serial block-face scanning electron microscopy to reconstruct three-dimensional tissue nanostructure. *PLoS Biology*, 2(11):e329, 2004.

[8] S. Geman and D. Geman. Stochastic relaxation, gibbs distributions, and the bayesian restoration of images. *IEEE Trans. Pattern Anal. Mach. Intell.*, 6:721–741, 1984.

[9] Chunming Li, Chenyang Xu, Changfeng Gui, and Martin D. Fox. Level set evolution without re-initialization: A new variational formulation. In *CVPR (1)*, pages 430–436. IEEE Computer Society, 2005.

[10] Lu Liu, David Raber, David Nopachai, Paul Commean, David Sinacore, Fred Prior, Robert Pless, and Tao Ju. Interactive separation of segmented bones in ct volumes using graph cut. In Dimitris N. Metaxas, Leon Axel, Gabor Fichtinger, and Gábor Székely, editors, *MICCAI (1)*, volume 5241 of *Lecture Notes in Computer Science*, pages 296–304. Springer, 2008.

[11] N. Otsu. A threshold selection method from gray-level histograms. *IEEE Transactions on Systems, Man and Cybernetics*, 9(1):62–66, January 1979.

[12] J. Stawiaski, E. Decencièere, and F. Bidault. Interactive liver tumor segmentation using graph cuts and watershed. In *Workshop on 3D Segmentation in the Clinic: A Grand Challenge II. Liver Tumor Segmentation Challenge. MICCAI, New York, USA. (2008).*, 2008.

[13] Wen-Bing Tao, Jin-Wen Tian, and Jian Liu. Image segmentation by three-level thresholding based on maximum fuzzy entropy and genetic algorithm. *Pattern Recognition Letters*, 24(16):3069–3078, 2003.

[14] Luc Vincent. Morphological grayscale reconstruction in image analysis: Applications and efficient algorithms. *IEEE Transactions on Image Processing*, 2:176–201, 1993.

[15] Luc Vincent and Pierre Soille. Watersheds in digital spaces: An efficient algorithm based on immersion simulations. *IEEE Trans. Pattern Anal. Mach. Intell.*, 13(6):583–598, 1991.

[16] Di Xiao, Wan Sing Ng, Charles B. Tsang, and Udantha R. Abeyratne. A region and gradient based active contour model and its application in boundary tracking on anal canal ultrasound images. *Pattern Recognition*, 40(12):3522–3539, 2007.